LAWRENCE
LIVERMORE
NATIONAL
LABORATORY

LLNL-PROC-490258

THE UPDATED LLNL-G3D GLOBAL P-WAVE VELOCITY MODEL AND ITS PERFORMANCE IN SEISMIC EVENT LOCATION

N. A. Simmons, S. C. Myers, G. Johannesson, E. Matzel

July 5, 2011

2011 Monitoring Research Review
Tucson, AZ, United States
September 20, 2011 through September 22, 2011

Disclaimer

This document was prepared as an account of work sponsored by an agency of the United States government. Neither the United States government nor Lawrence Livermore National Security, LLC, nor any of their employees makes any warranty, expressed or implied, or assumes any legal liability or responsibility for the accuracy, completeness, or usefulness of any information, apparatus, product, or process disclosed, or represents that its use would not infringe privately owned rights. Reference herein to any specific commercial product, process, or service by trade name, trademark, manufacturer, or otherwise does not necessarily constitute or imply its endorsement, recommendation, or favoring by the United States government or Lawrence Livermore National Security, LLC. The views and opinions of authors expressed herein do not necessarily state or reflect those of the United States government or Lawrence Livermore National Security, LLC, and shall not be used for advertising or product endorsement purposes.

THE UPDATED LLNL-G3D GLOBAL P-WAVE VELOCITY MODEL AND ITS PERFORMANCE IN SEISMIC EVENT LOCATION

Nathan A. Simmons, Stephen C. Myers, Gardar Johannesson and Eric Matzel
Lawrence Livermore National Laboratory

Sponsored by National Nuclear Security Administration

Contract No. DE-AC52-07NA27344/LL09-3Dseismic-NDD02

ABSTRACT

We have constructed a global-scale model of P-wave velocity with an emphasis on improving travel time prediction at both regional and teleseismic distances simultaneously. The *LLNL-G3Dv2* tomographic model is built within a spherical tessellation framework whereby irregular and discontinuous surfaces are explicitly represented. Fully 3-D ray tracing is employed for travel time prediction. The data consist of ~2.7 million P and Pn arrivals that are re-processed using our global multi-event locator known as *Bayesloc*. *Bayesloc* is a formulation of the joint probability distribution across multiple-event location parameters, including hypocenters, travel time corrections, pick precision, and phase labels. Modeling the whole multiple-event system results in accurate locations and an internally consistent data set that is ideal for tomography. Our recently developed inversion approach (called Progressive Multi-level Tessellation Inversion or PMTI) captures regional trends and fine details where data warrant. Using PMTI, we model multiple heterogeneity scale lengths without resorting to a user-defined parameter grids that can affect the resulting model. A number of features have emerged from the images including details of the underthrusted Arabian lithosphere beneath Eurasia (shown in our previous reports) and sharp details of subducted slabs around the world. Based on preliminary relocation tests, using *LLNL-G3Dv2* travel-time predictions typically reduces mislocation error for a set of globally distributed GT0-5 events by 30-45% (from ~10-11km using *ak135* to ~6-7 km) when a sufficient number of data are used. This work performed under the auspices of the U.S. Department of Energy by Lawrence Livermore National Laboratory under Contract DE-AC52-07NA27344. LLNL-PROC-490258

OBJECTIVES

The objective of this project is to generate a seamless model of the Earth's crust and mantle that is capable of accurately predicting regional and teleseismic travel times. The objective will further advance event monitoring capabilities, through self-consistent determination of seismic travel times that are necessary for accurate event location. The objective requires simultaneous modeling of detailed upper mantle heterogeneities to adequately predict regional phases such as P_n and lower mantle structures to predict teleseismic travel times. In addition to determining velocity structure, an efficient model design and computational framework must be established in order to routinely utilize the outcome model. In this report, we present our latest global 3-D P-wave velocity model and event location validation results.

RESEARCH ACCOMPLISHED

Employing a number of custom procedures described in previous Monitoring Research Review proceedings (e.g. Simmons et al. 2009a, 2010a) and the most recent peer-reviewed publications (e.g. Myers et al. 2011; Simmons et al. 2011), we have developed a revised global-scale P-wave velocity model that incorporates ~2.7 million re-processed regional and teleseismic travel times. We also performed exhaustive event location validation tests for a globally distributed set of events with Ground Truth (GT) levels of 5 or less. With this validation set of events, we typically find 30-45% improvement in median epicenter error when determining location on the basis of the most recent 3-D model (*LLNL-G3Dv2*) when more than ~20 arrivals are available. Although typical, this level of improvement depends on the number of supporting events and stations in a particular region (i.e. tomographic resolution).

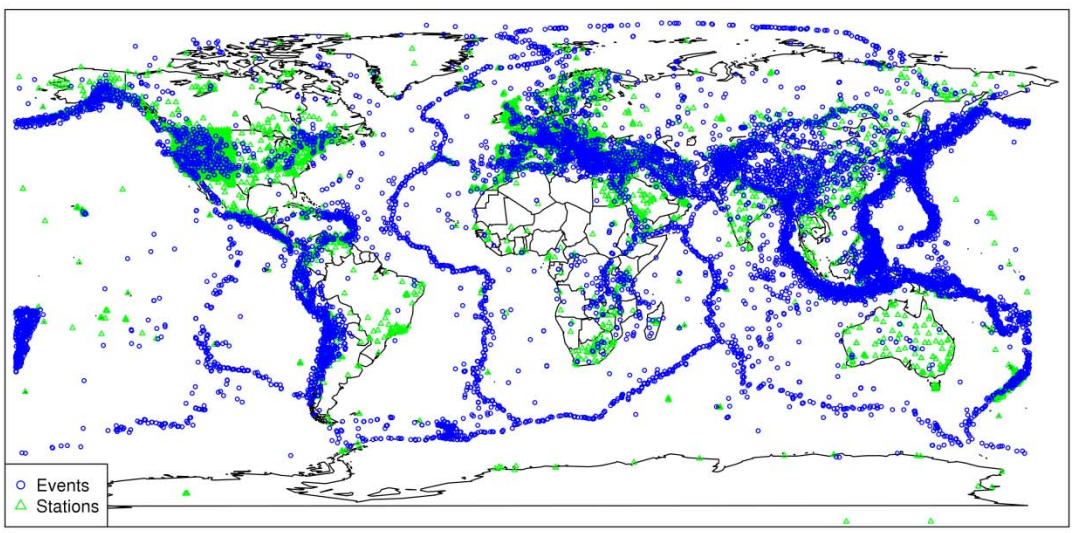

Figure 1. The dataset consists of ~13,400 seismic events (in blue) and ~8,000 stations (in green) providing a total of 3.4 million arrivals for phases: P, Pn, PcP, pP, sP, Sn, Pg, and Lg. The data are culled by the Bayeloc process and ~2.7 million P and Pn phases are used to develop the tomography model (*LLNL-G3Dv2*).

A New Global Dataset

Our raw (initial) compilation of travel time measurements come from a subset of our local database at Lawrence Livermore National Laboratory (Ruppert et al. 2005) and the publicly available Engdahl-van der Hilst-Buland (EHB) catalog (Engdahl et al. 1998). The most well-recorded global seismic events were selected nominally within 1° lateral bins and within 6 depth bins at 35, 75, 150, 300, 450 and 700 km depths. The dataset includes all GT5 and better events with >10 teleseismic or regional arrival picks. In total, there are approximately 3.4 million arrivals from ~13,400 seismic events recorded at ~8,000 stations around the globe (Figure 1). The vast majority of the data are teleseismic P-wave arrivals, but we also include the phases: Pn, PcP, pP, sP, Sn, Pg and Lg.

We have extended the Bayesloc method (originally designed to simultaneously locate a cluster of events) to global-scale multiple-event relocation (see Myers et al. 2007, 2009, 2011). The Bayesloc method simultaneously models all event hypocenters, regional travel time biases, path specific travel time errors, arrival time measurements and arrival time phase assignments within a Bayesian statistical framework. The process results in accurate event locations and travel times which are essential when generating a travel time tomography model (see Simmons et al. 2011). The updated Bayesloc procedure was performed on the aforementioned set of 13,400 events and 3.4 million arrivals to produce a new set of data for tomography with revised event locations (Figure 2). In summary, we find a median epicenter shift of 25.9 km from the bulletin locations. After Bayesloc processing, the travel time residual standard deviation drops from 1.87 to 1.35 seconds with respect to the AK135 model (Figure 3). Perhaps most importantly, we find clear regional trends in epicenter shift which has substantial impact on the resulting tomographic model.

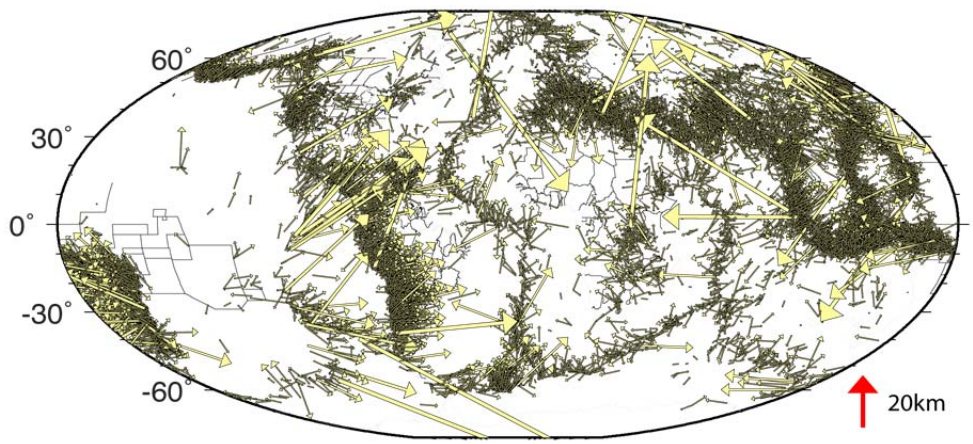

Figure 2. Epicenter shift vectors demonstrating the lateral re-location differences from the raw data and the Bayeloc processed data set. The Bayesloc process results in a median epicenter shift of 25.9 km with clear regional trends.

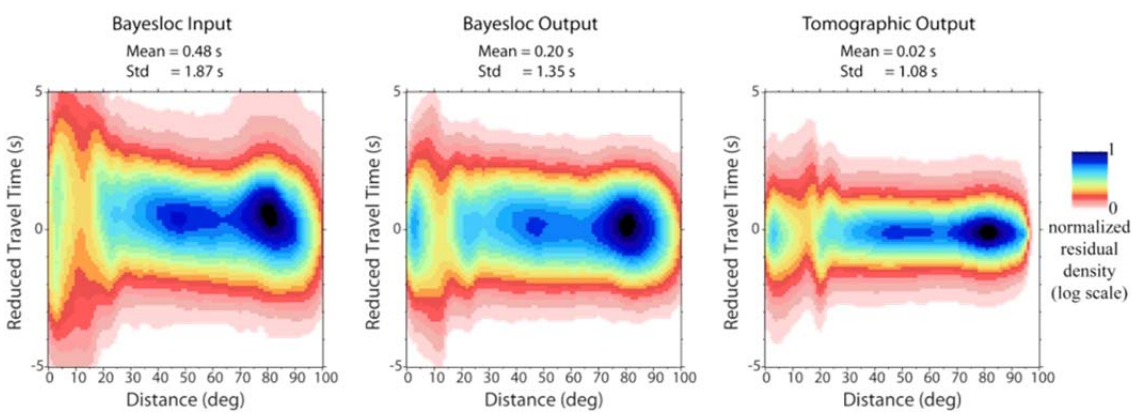

Figure 3. Travel time residual distribution for the ~2.7 million P and Pn arrivals. (LEFT) The initial bulletin data with respect to the AK135 model. (CENTER) The Bayesloc processed travel times with respect to the *ak135* model. (RIGHT) The Bayesloc processed travel times with respect to the *LLNL-G3Dv2* model presented in this report.

The *LLNL-G3Dv2* Model

The *LLNL-G3D* series of models are designed with the use of spherical tessellations whereby irregular and discontinuous surfaces can be explicitly represented (Ballard et al. 2009; Simmons et al. 2011). This style of explicit Earth representation is desirable given that we are simultaneously modeling regional- and global-scale velocity structures within a single, self-consistent model. Specifically, 3-D ray tracing is performed due to the extreme path-velocity dependencies arising at regional distances. Thus, we determine sensitivity via 3-D ray tracing (based on Zhao et al. 1992) while considering irregular discontinuity

structure and continuous media simultaneously. In addition, sensitivity is spread across broad depth zones and/or multiple model units to mitigate the issue of path-velocity interdependence as well as severe multi-pathing. See Simmons et al. (2011) for a complete description of the 3-D ray tracing procedures employed within the current study.

Rather than using a simple 1-D velocity model, we chose to create a starting P wave velocity model by combining components of existing models of the crust and mantle. There are many benefits of leveraging past work to design a first order starting model including: 1) providing constraints on regions with poor P-wave coverage, 2) mitigation of the non-linear relationship between ray paths and velocity structure, and 3) allowing for the determination of a new model that is most consistent with what is generally understood about the 3-D structure of the crust and mantle from decades of research.

For the crust, we use the 'Unified' crust model from the work of Pasyanos et al. (2004) and Steck et al. (2004) and Bassin et al. (2000). The crust model consists of 7 units including water, 3 sediment layers, and 3 crystalline crust layers. For the shallowest upper mantle, we use the results of the Regional Seismic Travel Time (RSTT) model described in Myers et al. (2010) including the sub-crustal velocity and mantle gradient terms. For the remainder of the mantle, we incorporated the results of the GyPSuM model (Simmons et al. 2010b). GyPSuM is a 3-D model of mantle S wave speed, P wave speed and density developed through simultaneous inversion of seismic and a suite of geodynamic constraints. The GyPSuM model represents the latest of a sequence of joint global modeling efforts described in Simmons et al. (2006, 2007, 2009b).

Numerous studies have independently concluded that significant topographic variations of the transition zone discontinuities exist. More specifically, it has been shown that the 410 km and 660 km discontinuities vary in depth by ±30 km or more over relatively short length scales (Lawrence and Shearer 2008). These variations may lead to incorrect 3-D ray path geometries, incorrect model sensitivity estimates, and therefore inaccurate velocity structure after tomographic inversion is performed. For this reason, we adjusted the depths of the 410 and 660 according to the transition zone discontinuity topographies determined in the global high-resolution SS precursor study of Lawrence and Shearer (2008). In addition, the model explicitly characterizes Earth's asphericity in accord with the WGS84 reference ellipsoid and the expected hydrostatic shape of mantle layers and the core-mantle boundary.

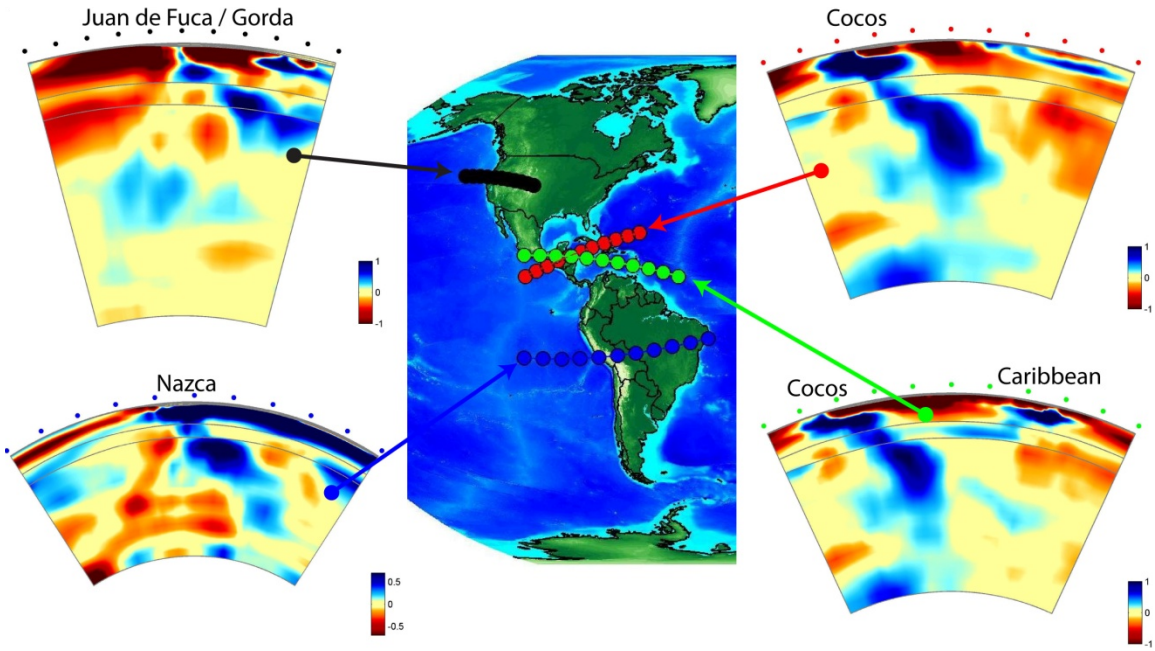

Figure 4. Cross-sections through the *LLNL-G3Dv2* model showing subducting slabs beneath the Americas.

As noted in previous reports, the tessellation-based model design is hierarchical since the mesh is a product of subdividing a base level tessellation a number of times. One of the major outstanding issue in seismic tomography is the uneven sampling of seismic data and the differing wavelengths of actual seismic heterogeneity. These issues make it difficult to design an appropriate mesh. Thus, we have developed an inversion process called Progressive Multilevel Tessellation Inversion (PMTI) that exploits the hierarchical nature of the tessellation-based design and allows the data to determine the level of model complexity, without user bias. PMTI serves as an alternative to existing multiresolution approaches and we have demonstrated that the process robustly images regional trends while allowing localized details to emerge where resolution is sufficient (see Simmons et al. 2011 for more details). Using the PMTI process, we update the aforementioned starting model to produce the P-wave velocity model shown in Figures 4-5.

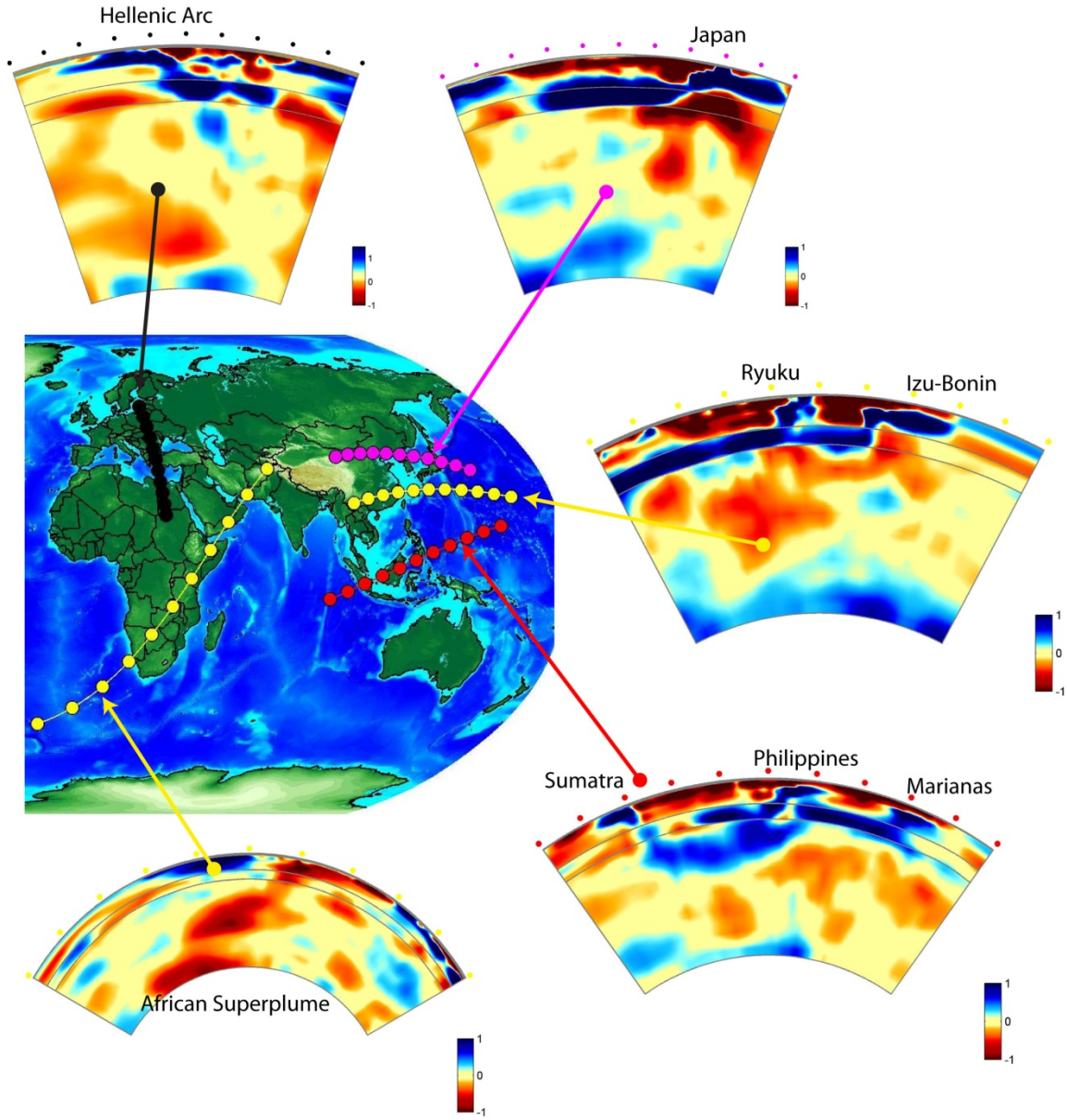

Figure 5. Cross-sections through the *LLNL-G3Dv2* model showing subducting slabs beneath Eurasia and Indonesia, as well as the superplume beneath Africa. Color scales change from one frame to the next (denoted by the colorbars) and all values are in terms of percent Vp variation relative to the mean model with depth.

The resulting image (Figure 4-5) reveals a number of subducted slabs around the world, including: i) details of the Juan de Fuca, Cocos, and Nazca plates beneath the Americas, ii) the Pacific and Phillipine plates along the western margins of the Pacific, iii) the African plate subducting beneath Europe along the Hellenic Arc, iv) interaction of the Australian, Phillipine and Pacific plates beneath Indonesia, and v) superplumes beneath the Pacific and Africa. Countless other features emerge from the images but further discussion is beyond the scope of this report.

Resolution tests were carried out using the inversion procedures discussed above. Our synthetic model is a combination of two checkerboards summed together to create large-scale regional trends combined with more local detail (Figure 6). The smallest checkerboard squares are 5° × 5° in dimension and the pattern was repeated with opposite signs in each of the 31 inversion layers from the Moho to the core-mantle boundary. Therefore, we developed a single model for the entire depth range of the mantle rather than testing one layer at a time (Figure 6 and the left column of Figure 7). In addition, we carried out resolution tests with a single layer at a time approach which is the standard approach to compare the two styles (Figure 7). Not surprisingly, the "one layer at a time" approach shows better input model recovery especially where data densities are low (e.g beneath the Pacific Ocean and near the South Pole).

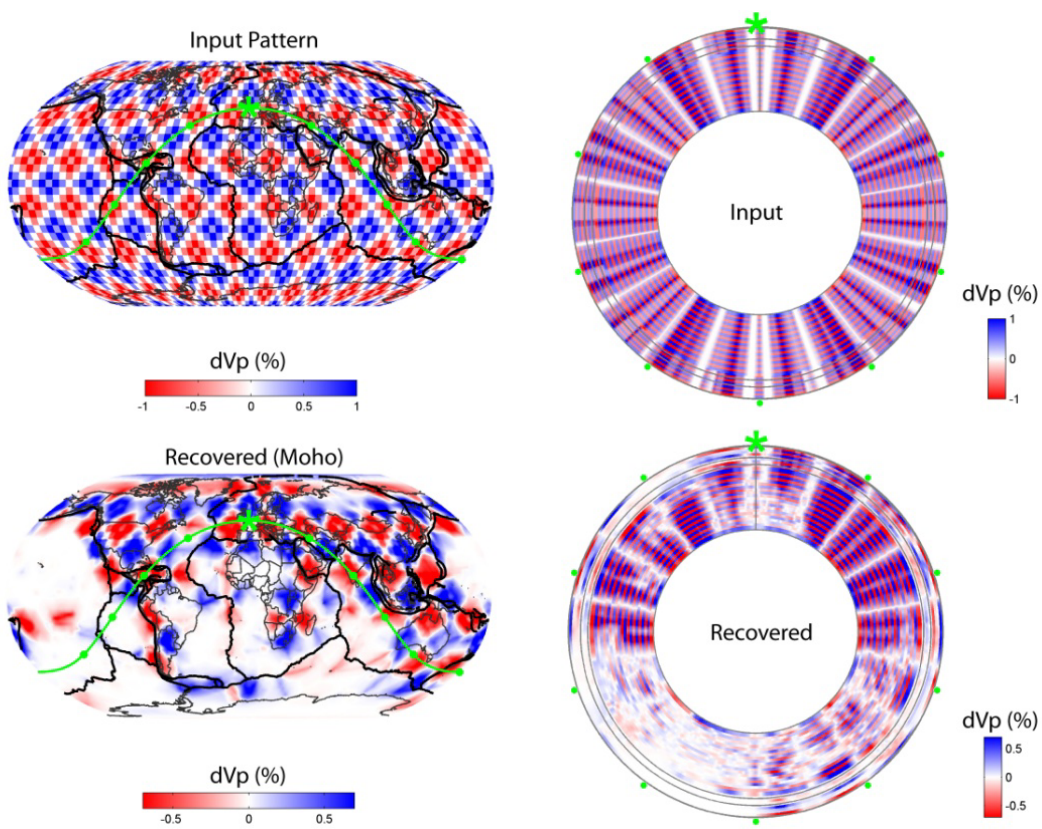

Figure 6. Checkerboard test input pattern, recovery at the Moho, and recovery along the green, 360-degree cross-section.

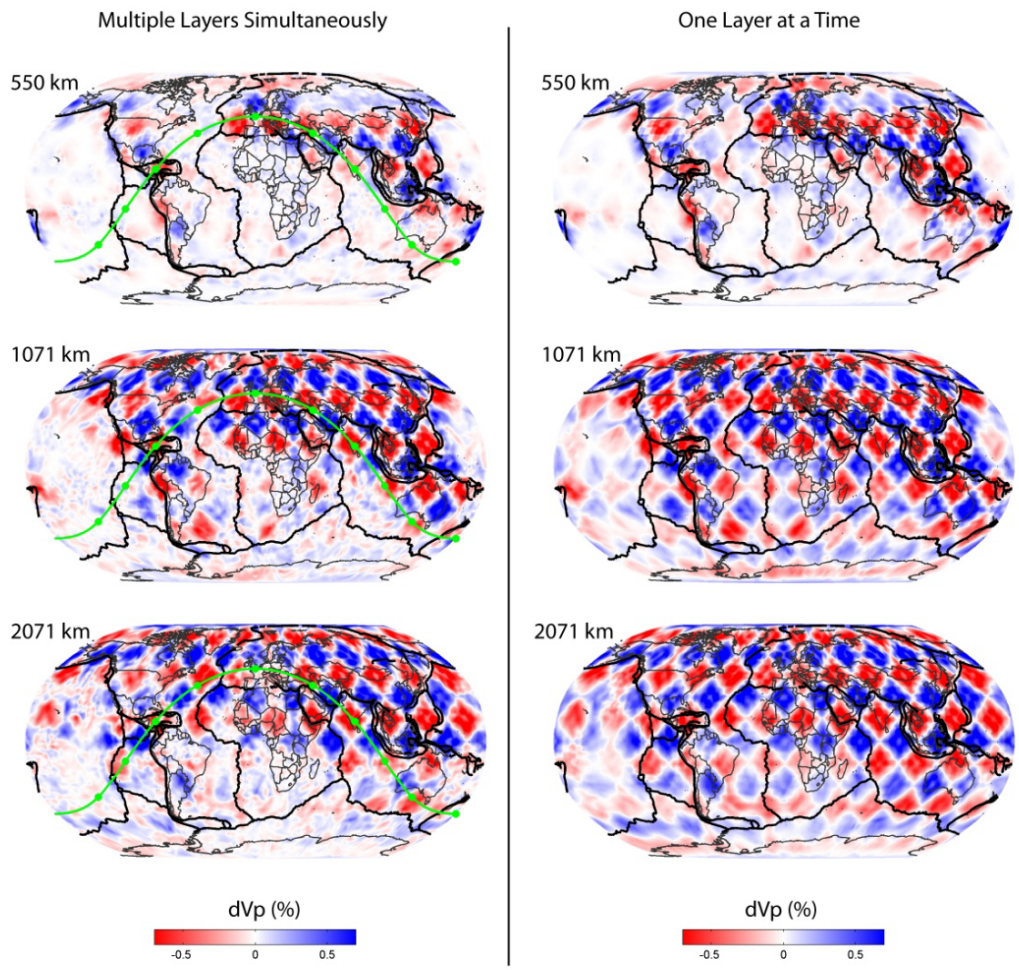

Figure 7. Resolution test recovery at 3 specific depths for the case with multiple layers (left column) and the case with a single layer at a time (right column) for comparison.

Global Event Location

For location validation, we selected 116 of the most well-recorded GT5 (or better) events within 5-degree bins. Each event that maximizes the number of arrivals or network coverage (minimizes station azimuthal gap) at regional or teleseismic distances was selected. As a result, up to 4 distinct events may be selected within each 5-degree bin. The events are globally distributed, but the majority of events are in Eurasia (Figure 8). Data from the 116 events were excluded from the tomographic inversion to produce a validation version of *LLNL-G3Dv2* to prevent circularity. For each event, we randomly selected specific numbers of P and Pn arrival times to be used for event location (ranging from 0 to 100 arrivals). For each event data sampling, we required that there be at least 5 arrivals and that enough data were available to produce at least 10 distinct realizations of arrival times.

All relocations were determined using the *Bayesloc* algorithm in "single-event" mode – no travel time corrections, assessment of travel time error, or phase labeling error – and without significant assumed prior information about the event. For the 1-D model case, locations were determined based on *ak135* travel times. For the 3-D case, we used an iterative approach with the steps: i) find the 1-D location, ii) adjust the arrival times based on the difference between *ak135* and the computed *LLNL-G3Dv2* travel times , and iii) relocate using *Bayesloc*. Effectively, this process removes the 3-D travel time signal from the data given a location that is "in the ballpark" (i.e. 1-D location) and then relocate once again assuming a 1-D background velocity model (*ak135*).

Figure 9 shows a summary of the event location validation results. The results are demonstrated by binning the event realizations according to the number of P and Pn used, and the median epicenter mislocation error (in km) was determined for all events located with the specified number of data. We find that, in most cases, using the 3-D model produces more accurate locations than the *ak135* model. More specifically, in 98% of all the cases, the 3-D model improved location accuracy. The exceptions occur for relocations using few data, where both 1-D and 3D models result in mislocations of many tens of km.

Aside from cases with very few data, we find the least improvement when only P arrivals are used (Figure 10). With sufficient data, the median mislocation using *ak135* is ~9-10 km whereas *LLNL-G3D* mislocates by ~7 km. The ~20-30% improvement is not surprising since *ak135* is a good global average model for teleseismic arrivals by design. In cases where only Pn arrivals are used, the 3-D model improves location more considerably more (~11 km to ~6-7 km, ~35-45%) owing to significant 3-D heterogeneities on the regional scale.

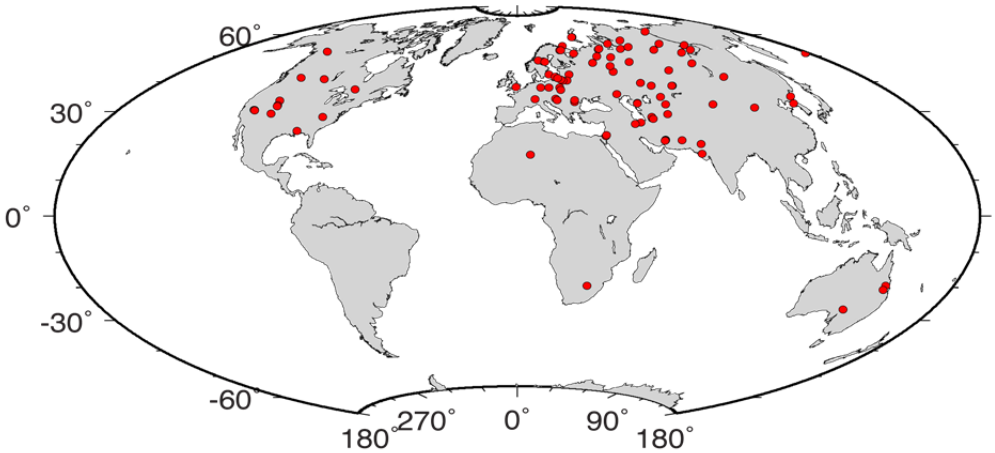

Figure 8. Events used for location validation. See text for details.

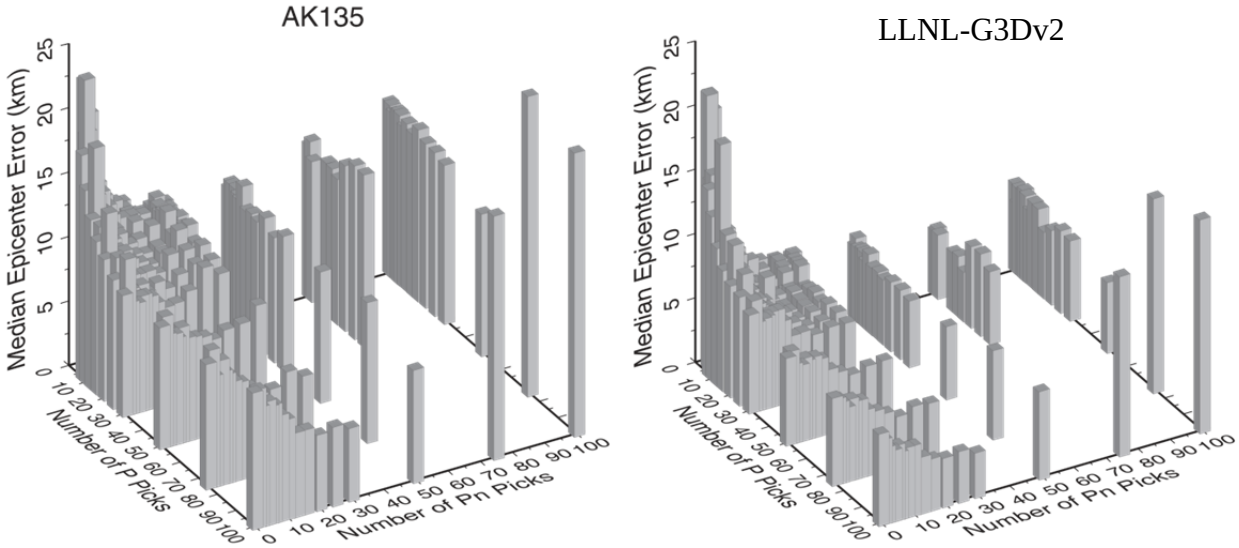

Figure 9. Median epicenter error for all of the realized validation events (see text). (left) Epicenter errors as a function of the number of P and Pn picks used assuming the AK135 1-D velocity model. (right) using the *LLNL-G3Dv2* model.

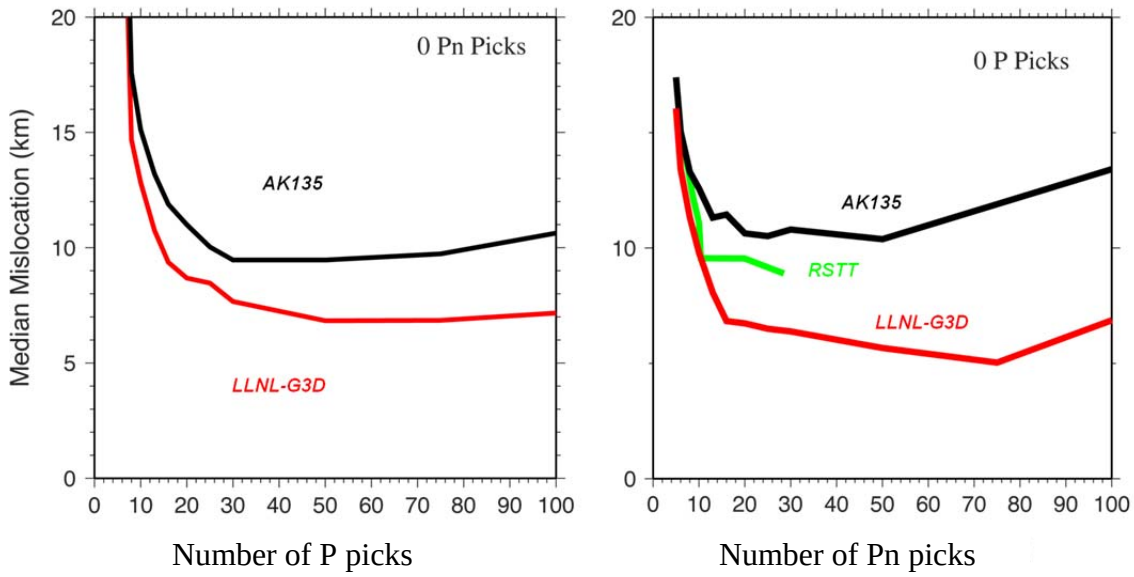

Figure 10. Median epicenter mislocation for the cases where all data are either P picks (left) or Pn picks (right) where the other phase is excluded.

CONCLUSIONS AND RECOMMENDATIONS

We have constructed a new version of the *LLNL-G3D* (version 2) global-scale model of P-wave velocity that is a seamless model of Earth's crust and upper mantle. The *LLNL-G3Dv2* tomographic model is constructed with ~2.7 million P and Pn arrivals that are re-processed using our global multi-event locator known as *Bayesloc*. With *LLNL-G3Dv2*, the large set of globally distributed P wave data are predicted within 1.08 seconds standard deviation compared to 1.87 seconds for *ak135* (~67% variance reduction). The image provides sharp details of subducted slabs around the world, including those most often only seen with detailed regional studies, as well superplumes and many other geologically significant features.

Based on these preliminary tests, *LLNL-G3Dv2* typically reduces mislocation error for a set of 116 globally distributed GT0-5 events by 30-45% (from ~10-11km using *ak135* to ~6-7 km) when a sufficient number of data are available. The 3-D model predicts locations that are more accurate than *ak135* in 98% of the cases considered. Most notably, the 3-D model more substantially improves the location of events when no P wave arrivals are used in the location (Pn only). This result is expected due to the fact that *ak135* was designed to be an average Earth model to compute average P-wave velocity times at teleseismic distances.

We find that regions with low seismicity levels and light station coverage produce the worst location predictions with the 3-D model owing to the limited understanding of the velocity structures. The extreme example is in Northwest Asia/Eastern Europe (typically ~18% epicenter location improvement) compared to other regions such as western North America (typically >45% location improvement). The limitation of a specific type of seismic information (e.g. P and Pn arrivals) in a particular region suggest that other forms of data must be incorporated when generating a travel time model suitable for accurate event monitoring. This should be the focus of future work.

Prepared by LLNL under Contract DE-AC52-07NA27344.

REFERENCES

Ballard, S., J. R. Hipp and C. J. Young (2009), Efficient and accurate calculation of ray theory seismic travel time through variable resolution 3D Earth models, *Seis. Res. Lett.*, *80*(6), 990-1000.

Bassin, C., G. Laske, and G. Masters (2000), The current limits of resolution for surface wave tomography in North America, *Eos Trans*. AGU, 81, F897.

Engdahl, E. R., R. van der Hilst and R. Buland (1998), Global teleseismic earthquake relocation with improved travel times and procedures for depth determination, *Bull. Seis. Soc. Amer*., *88*(3), 722-743.

Lawrence, J. G., and P. M. Shearer (2008), Imaging mantle transition zone thickness with SdS-SS finite-frequency sensitivity kernels, *Geophys. J. Int*., *174*, 143–158, doi:10.1111/j.1365-246X.2007.03673.x.

Myers, S. C., G. Johannesson and W. Hanley (2007), A Bayesian hierarchical method for multiple-event seismic location, *Geophys. J. Int*., *171*, 1049-1063.

Myers, S. C., G. Johannesson and W. Hanley (2009), Incorporation of probabilistic seismic phase labels into a Bayesian multiple-event seismic locator, *Geophys. J. Int*., *177*, 193-204.

Myers, S. C., G. Johannesson and N. A. Simmons (2011), Global-scale P-wave tomography optimized for prediction of teleseismic and regional travel times for Middle East events: 1. Data set development, *J. Geophys. Res*., 116, B04304, doi:10.1029/2010JB007967.

Myers, S. C., M. L. Begnaud, S. Ballard, M. E. Pasyanos, W. S. Phillips, A. L. Ramirez, M. S. Antolik, K. D. Hutchenson, J. J. Dwyer, C. A. Rowe and G. S. Wagner (2010a), A crust and upper-mantle model of Eurasia and North Africa for P_n travel-time calculation, *Bull. Seis. Soc. Amer*., *100*(2), 640-656.

Pasyanos, M. E., W. R. Walter, M. P. Flanagan, P. Goldstein, and J. Bhattacharyya (2004), Building and testing an a priori geophysical model for Western Eurasia and North Africa, Pure Appl. Geophys., 161, 235–281, doi:10.1007/s00024-003-2438-5.

Ruppert, S., D., Dodge, A. Elliott, M. Ganzberger, T. Hauk and E. Matzel (2005). Enhancing seismic calibration research through software automation and scientific information management, in *Proceedings of the 27th Seismic Research Review: Ground-Based Nuclear Explosion Monitoring Technologies*, LA-UR-05-6407, Vol. 2.

Simmons, N. A., A. M. Forte, and S. P. Grand (2006), Constraining mantle flow with seismic and geodynamic data: A joint approach, Earth Planet. Sci. Lett., 246, 109–124, doi:10.1016/j.epsl.2006.04.003.

Simmons, N. A., A. M. Forte, and S. P. Grand (2007), Thermochemical structure and dynamics of the African superplume, Geophys. Res. Lett., 34, L02301, doi:10.1029/2006GL028009.

Simmons, N. A., S. C. Myers and A. Ramirez (2009a), Multi-resolution seismic tomography based on a recursive tessellation hierarchy, in *Proceedings of the 2009 Monitoring Research Review: Ground-Based Nuclear Explosion Monitoring Technologies*, LA-UR-09-05276, Vol. 1, pp. 211-220.

Simmons, N. A., A. M. Forte, and S. P. Grand (2009b), Joint seismic, geodynamic and mineral physical constraints on three-dimensional mantle heterogeneity: Implications for the relative importance of thermal versus compositional heterogeneity, Geophys. J. Int., 177, 1284–1304, doi:10.1111/j.1365-246X.2009.04133.x.

Simmons, N. A., S. C. Myers and G. Johannesson (2010a), Global-scale P-wave tomography designed for accurate prediction of regional and teleseismic travel times for Middle East events, in *Proceedings of the 2010 Monitoring Research Review: Ground-Based Nuclear Explosion Monitoring Technologies*, LA-UR-10-05578, Vol. 1, pp. 211-220.

Simmons, N. A., A. M. Forte, L. Boschi, and S. P. Grand (2010b), GyPSuM: A joint tomographic model of mantle density and seismic wave speeds, J. Geophys. Res., 115, B12310, doi:10.1029/2010JB007631.

Simmons, N. A., S. C. Myers and G. Johannesson (2011), Global-scale P-wave tomography optimized for prediction of teleseismic and regional travel times for Middle East events: 2. Tomographic inversion, *J. Geophys. Res*., 116, B04305, doi:10.1029/2010JB007969.

Steck, L. K., C. A. Rowe, M. L. Begnaud, W. S. Phillips, V. L. Gee, and A. A. Velasco (2004), Advancing seismic event location through difference constraints and three-dimensional models, paper presented at *26th Seismic Research Review: Trends in Nuclear Explosion Monitoring*, Natl. Nucl. Security Admin., Orlando, Fla.

Zhao, D., A. Hasegawa, and S. Horiuchi (1992), Tomographic imaging of P and S wave velocity structure beneath northeastern Japan, *J. Geophys. Res*., *97*, 19909–19928.